

THE 4TH INTERNATIONAL CONFERENCE ON ALUMINUM ALLOYS

Effect of Mg Addition on Precipitation Hardening of Al-Li-Cu-Zr Alloys Containing Ag

Shoichi Hirosawa¹, Tatsuo Sato¹, Akihiko Kamio¹,
Kazunori Kobayashi² and Toshimasa Sakamoto²

1. Dept. of Metallurgical Engineering, Tokyo Institute of Technology,

2-12-1 O-okayama, Meguro-ku, Tokyo 152, Japan.

2. Alithium Ltd., 2-2-2 Ogoso-Higashi, Yokkaichi-shi, Mie 510, Japan.

Abstract

The Al-Li-Cu-Mg-Zr alloy containing Ag, known as WeldaliteTM049 alloy, exhibits ultra-high mechanical strength caused by homogeneous precipitation of the T₁(Al₂CuLi) phase, and shows excellent weldability with marked natural aging response due to high Cu content. In particular, small addition of Mg has a significant role to attain these characteristic properties. The present work aims to investigate the effect of small amount of Mg addition on precipitation hardening of Al-Li-Cu-Ag-Mg-Zr alloy at various aging temperatures. The microstructures observed with transmission electron microscopy and hardness changes indicate the pronounced effects of Mg addition. In the temperature range from R.T. to 373K small amount of Mg stimulates precipitation of GP(1) zone, resulting in the marked age-hardening. At the more elevated temperatures, however, the Mg addition results in the change in the predominant precipitates from the GP(2) zone and/or θ' phase (Mg-free alloy) to the T₁ phase (Mg-containing alloy). The mechanism for the effect of Mg addition is discussed based on both the nucleation of precipitates and the vacancy-solute atom interaction.

Introduction

The application of a low density and high modulus Al-Li alloy over a wide range of structural components requires both desirable strength-ductility combination and good weldability. From these alloy design concepts, WeldaliteTM049 alloy was developed by Martin Marietta Corporation, having a high Cu/Mg(mass%) ratio and small addition of Ag with a normal composition of Al-(4.5-6.3)Cu-1.3Li-0.4Ag-0.4Mg-0.14Zr (in mass%). The ultra-high strength of the alloy (yield strength of ~ 690 MPa) in either T8(stretch and artificial aging) or T6(no stretch and artificial aging) temper is attributed to homogeneous precipitation of the T₁ (Al₂CuLi) phase with a presence of δ' (Al₃Li), GP zone, θ' (Al₂Cu) and S' (Al₂CuMg) phases. In addition, this alloy exhibits excellent weldability due to both the marked aging response in the T4(no stretch and natural aging) temper and a large amount of eutectic compounds to heal hot tears formed during the welding operation. The high mechanical strength in the T4 temper (yield strength of ~ 440 MPa) arises from a combination of refined GP zones and the δ' precipitates, without any other phases recognized.

Small additions of Ag and Mg are utilized to stimulate fine distribution of the T₁ phase in the artificial aging. Polmear *et al.*[1] reported that small amounts of Ag and Mg have marked effects to increase the age-hardening response for Al-Cu alloys, resulting from fine dispersion of hexagonal-shaped thin plates of the Ω phase on the $\{111\}_\alpha$ planes. Furthermore, Taylor *et al.*[2] proposed that the nucleation of the Ω phase takes place on the fine Mg₃Ag particles formed on the $\{111\}_\alpha$ planes. This seems to be applicable to explain the nucleation of the T₁ phase in Weldalite™049 alloy.

The goal of this work is to examine the role of small amount of Mg addition on the precipitation hardening of Weldalite™049 alloy in the temperature range from R.T.(room temperature) to 523K. The predominant phases effective to increase mechanical strength at various aging temperatures and time were identified using transmission electron microscope (TEM) technique. The measurement of precipitate size distributions was also performed to determine precipitate populations and formation kinetics of each phase. From these results, the mechanism for the effect of Mg addition is discussed based on both the nucleation of precipitates and the vacancy-solute atom interaction.

Experimental procedure

The alloys were prepared from high-purity materials in argon gas atmosphere. The chemical composition of the alloys is shown in Table 1. The ingots were homogenized at 723K for 36.4ks, then scalped, and hot and cold-rolled to 1.6mm thick sheets. All of the specimens were solution-treated at 778K for 1.8ks in a salt bath, and followed by water quenching. The aging treatment was carried out in an oil bath at temperatures from R.T. to 523K for various periods. Hardness measurements were made on the as-polished specimens using a Micro Vickers testing machine with a 500g load. The specimens for the tensile test were prepared from the 1.0mm thick sheets in the longitudinal direction with a gauge length of 25mm. Tensile tests were performed with a Instron-type tensile test machine at a strain rate of 1.3×10^{-4} /s. The specimens for transmission electron microscopy (TEM) analysis were prepared by the twin-jet polishing technique in a solution of 25 vol.% nitric-acid and 75 vol.% methanol at about 250K. TEM observation was carried out at an accelerating voltage of 200kV using a JEM200CX transmission electron microscope.

Table 1 Chemical compositions of Weldalite and Mg-free alloys (mass%).

| | Cu | Mg | Ag | Li | Zr | Si | Fe | Ti | Al |
|-----------|------|-------|------|------|------|------|------|------|------|
| Weldalite | 5.52 | 0.50 | 0.39 | 1.36 | 0.16 | 0.08 | 0.05 | 0.03 | bal. |
| Mg-free | 5.65 | 0.002 | 0.38 | 1.35 | 0.15 | - | - | - | bal. |

Results

1. Aging behavior at R.T. to 373K

Fig.1 shows the isothermal aging curves of hardness for Weldalite and Mg-free alloys aged at R.T. to 373K. With increasing aging time Weldalite alloy displays a rapid and pronounced hardening to attain a constant value at each aging temperature. On the other hand, although the hardness increment is obviously retarded, Mg-free alloy also shows increased age-hardening to attain the almost identical values of hardness after extended incubation periods (see curves of 373K shown in Fig.1).

Fig.2(a) shows a bright field TEM image for Weldalite alloy aged at R.T. for 864ks. The corresponding diffraction pattern exhibits diffuse continuous streaks and superlattice reflections, showing the presence of a combination of refined GP(1) zones and the δ' phase. It is well known that the δ' phase is rapidly formed from the supersaturated solid solution during or just after water quenching, whereas the growth of the δ' phase occurs to a lesser extent at low temperatures such as R.T.. Therefore, the marked natural aging response of WeldaliteTM049 alloy seems to be mainly due to the growth of GP(1) zones. In contrast, the microstructure of Mg-free alloy aged at R.T. for 864ks reveals almost no phases except the δ' phase. However, increased aging time ($\sim 2.7 \times 10^5$ ks) stimulates the formation of GP(1) zones with the image contrast due to the strain field (Fig.2(b)). This implies that small addition of Mg has a significant role to produce a rapid natural aging response for WeldaliteTM049 alloy associated with GP(1) zones. The similar results are also obtained for both Weldalite and Mg-free alloys aged at 373K. Thus, the addition of small amount Mg is found to accelerate the precipitation of GP(1) zones resulting in the faster age-hardening. In this aging temperature range the T₁ phase is not observed.

The tensile properties of two alloys are well correlative with the hardening behavior. The stress-strain curves for two as-quenched alloys reveal serrated flow as frequently observed in the plastic deformation of Al-Li alloys. However, after natural aging for 86.4ks the stress-strain curve becomes smooth only for Weldalite alloy, in contrast, that of Mg-free alloy still represents serrated flow. The disappearance of the serrated flow in the naturally aged WeldaliteTM 049 alloy is also attributed to the effect of Mg addition.

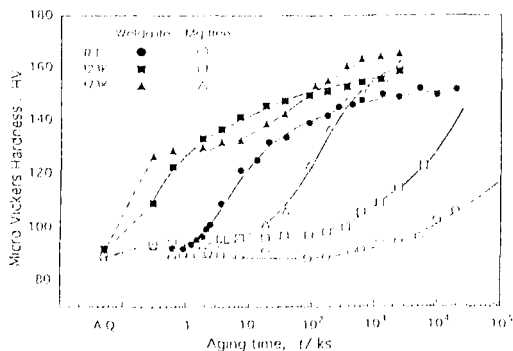


Fig.1 Isothermal aging curves of hardness for Weldalite and Mg-free alloys aged at R.T. to 373K.

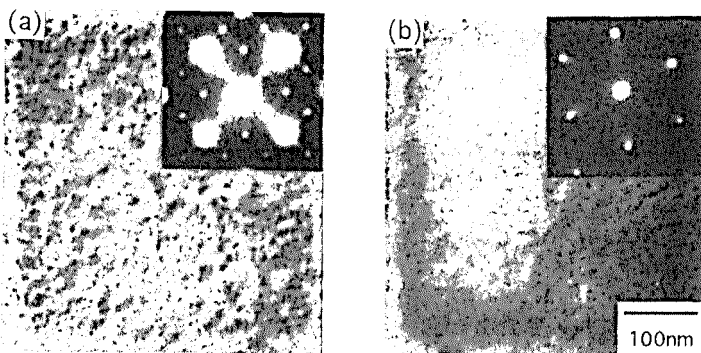


Fig.2 Electron micrographs with diffraction pattern for (a) Weldalite alloy aged at R.T. for 864ks and (b) Mg-free alloy aged at R.T. for $\sim 2.7 \times 10^5$ ks.

2. Aging behavior at 403 to 523K

Fig.3 illustrates the isothermal aging curves of hardness for Weldalite and Mg-free alloys aged at 403 to 463K. The results indicate that the small amount of Mg reduces the aging time to reach peak hardness with a marked increase in peak hardness. This can be explained in terms of the change in the microstructures produced during aging. The predominant strengthening precipitates identified by TEM for various aging conditions are listed in Table 2. After aging at 433K for 36ks, for example, both Weldalite and Mg-free alloys exhibit microstructures containing GP(1) zones and the δ' phases. However, after aging for 346ks Weldalite alloy alone produces the T_1 phase with a presence of δ' phase and GP(2) zone, whereas in Mg-free alloy the T_1 phase is not detected until the time of overaging (1.9×10^4 ks) (Fig.4(a),(b),(c)). The similar results are also demonstrated for two alloys aged at 463K. Thus, the addition of Mg causes the change in the major strengthening phase from the GP zones and/or θ' phase to the T_1 phase, resulting in the marked acceleration of the T_1 phase formation. Mg-containing precipitates such as GPB zone and the S' phase are not detected in Weldalite alloy, except for small amounts of GPB(2) zones observed in the aging at 403K for 9.7×10^3 ks.

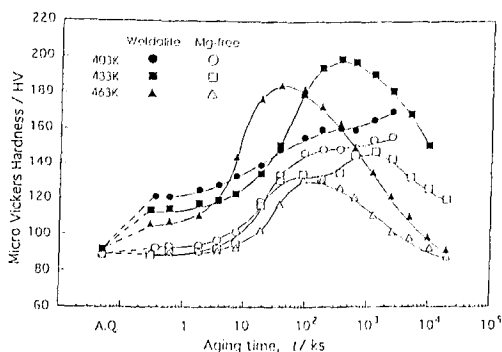


Fig. 3 Isothermal aging curves of hardness for Weldalite and Mg-free alloys aged at 403 to 463K.

Table 2 Precipitates observed in Weldalite and Mg-free alloys aged at R.T to 523K.

| Temp. | Time/ks | Weldalite | Mg-free |
|-------|----------------------|---------------------------------|-------------------------------|
| R.T. | 8.6×10^{-2} | δ' GP(1) | δ' |
| | 2.7×10^4 | --- | (δ') GP(1) |
| 373K | 1.8×10^3 | δ' GP(1) | δ' GP(1) |
| 403K | 1.8×10^3 | δ' GP(1) | δ' GP(1) |
| | 9.7×10^3 | δ' GP(2) T_1 GPB(2) | --- |
| 433K | 3.6×10^3 | δ' GP(1) | δ' GP(1) |
| | 3.5×10^2 | δ' GP(2) T_1 | δ' GP(2) |
| | 1.9×10^4 | --- | (δ') θ' T_1 |
| 463K | 7.2 | T_1 | (δ') GP(2) |
| | 3.6×10^3 | T_1 | δ' GP(2) T_1 |
| | 1.9×10^4 | T_1 | (δ') θ' T_1 |
| 523K | 9.0×10^{-1} | T_1 | T_1 |
| | 1.8 | T_1 | T_1 |

Discussion

1. Mechanism for Mg addition at R.T. to 373K

In the temperature range from R.T. to 373K, an obvious difference in the aging response between Weldalite and Mg-free alloys (Fig.1) can be mainly explained in terms of the change in the precipitation rate of GP(1) zones. It is well known that the addition of small amount of Mg to Al-Cu alloys accelerates the formation of GP(1) zones resulting in the faster natural age-hardening, whereas the additions of other elements such as Cd, In and Sn lower the natural age-hardening rate by suppressing the formation of GP(1) zones. Entwistle *et al.*[3] proposed that Cu/Mg/vacancy complexes are formed at the initial stage of aging due to a high Mg-vacancy binding energy, and promote copper diffusion necessary to form GP(1) zones by a process of reshuffling of the associated vacancies. Furthermore, Wyss *et al.*[4] suggested that

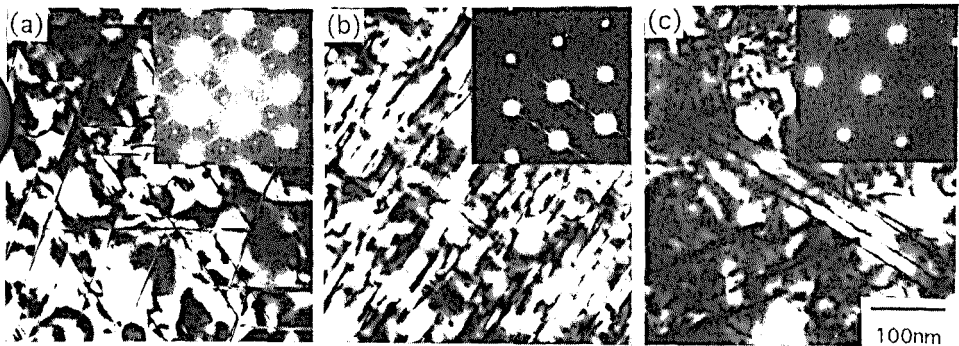


Fig.4 Electron micrographs with diffraction pattern for (a) Weldalite alloy aged at 433K for 346ks and Mg-free alloys aged at 433K for (b)346ks and (c) 1.9×10^4 ks.

the formation of Mg-vacancy clusters enhances nucleation of GP(1) zones by increasing the number of nucleation sites or increasing the nucleation rate. It is likely that the similar mechanisms for Mg addition are applicable to the Li-containing WeldaliteTM049 alloy.

In general, the diffusion coefficient of Cu in Al is given as [5]

$$D_{Cu} = A \exp(-E_m/kT_a) \exp(-E_f/kT_q), \quad (1)$$

where E_m and E_f are the activation energies for the migration and formation of vacancies, T_a and T_q are the aging and solution treatment temperatures, k is Boltzmann's constant and A is a constant. However, if the quench operation is carried out quickly enough to retain the vacancy concentration associated with T_q , the clustering process of Cu atoms should be mainly governed by the first exponential term because an activation energy E_f for the formation of vacancies becomes negligible. In fact, an activation energy for the formation of GP zones in as-quenched Al-4%Cu alloy, 0.54eV, agrees well with an activation energy E_m for the migration of vacancies, 0.51eV.

In the present study, the activation energies for the formation of GP(1) zones in Weldalite and Mg-free alloys can be estimated by utilizing the isothermal aging curves of hardness (Fig.1). That is, if the hardness increment is proportional to the volume fraction of the formed GP(1) zones to attain identical values of hardness, Arrhenius plots of the reciprocal time $1/t$, obtained from the cross-cut at 50% age-hardening from as-quenched hardness, would provide the activation energies for the formation of GP(1) zones. In fact, from the slope of each straight line through the Arrhenius plots in Fig.5, the activation energies are assessed to be 0.38eV and 0.59eV for Weldalite and Mg-free alloys,

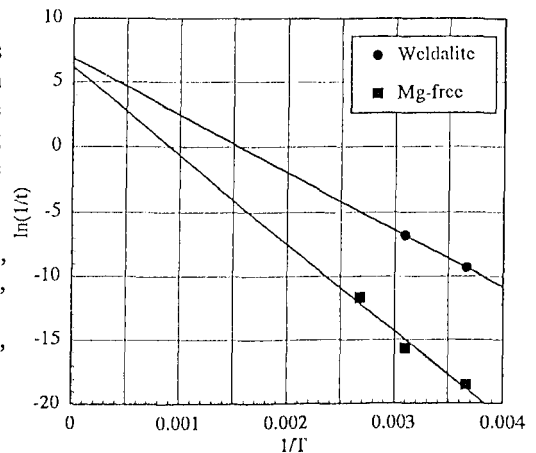


Fig.5 Arrhenius plots of reciprocal time to 50% age-hardening from as-quenched hardness against reciprocal temperatures for Weldalite and Mg-free alloys.

respectively. In contrast, the jump frequency of vacancies or the nucleation frequency of GP(1) zones, given by an intercept on the $\ln(1/t)$ axis in Fig.5, is found to be approximately equal in two alloys. These results indicate that small amount of Mg in Weldalite™049 alloy remarkably accelerate the growth rate of GP(1) zones, resulting in a decreased activation energy for the formation, whereas the number of nucleation sites or the nucleation rate is not affected. The similar results are also obtained for the cross-cut at 30% age-hardening, the activation energy for the formation of GP(1)zone in Weldalite alloy (0.40eV) is rather smaller than that in Mg-free alloy (0.56eV), which is almost equal to the activation energy for the migration of vacancies (0.51eV).

Table 3 The calculated enthalpy of solution at infinite dilution, ΔH^0 in kJ/mol[8].

| | Al | Li | Cu | Mg | Ag | Cd | In | Sn |
|----|-----|-----|-----|-----|-----|-----|-----|-----|
| Al | | -15 | -34 | -7 | -17 | 12 | 24 | 14 |
| Li | -13 | | -19 | -1 | -55 | -43 | -41 | -56 |
| Cu | -28 | -18 | | -15 | 8 | 2 | 8 | -3 |
| Mg | -8 | -1 | -20 | | -42 | -22 | -14 | -31 |
| Ag | -18 | -65 | 10 | -40 | | -8 | -5 | -10 |

These can be interpreted in terms of the Cu/Mg/vacancy complexes diffusion proposed by Entwistle *et al.*[3]. Although a number of arguments have been done on a Mg-vacancy interaction, the relatively high Mg-vacancy binding energy compared with Cu-vacancy binding energy (values of 0.19eV[6] and 0.36 ± 0.04 eV[7] are measured) will contribute to form numerous Mg/vacancy pairs during the solution treatment. These pairs persist through the quench operation, and might acquire copper atoms because of the strong Mg-Cu interaction predicted based on the calculated enthalpy of solution at infinite dilution. Table 3 shows the extracted values from the lists reported by Niessen *et al.*[8]. Therefore, the diffusivity of copper atoms in Weldalite™049 alloy increases due to the increased frequency of Cu atoms to encounter vacancies through Mg atoms. In contrast, the elements having high binding energies with vacancies such as Cd(0.18eV), In(0.25eV) and Sn(0.22eV) do not have so strong interactions between Cu atoms as shown in Table 3, thereby inhibit the formation of GP(1) zones by trapping vacancies available for Cu diffusion.

2. Mechanism for Mg addition at 403 to 523K

On the other hand, in the temperature range from 403 to 523K, the precipitate size distributions and precipitate densities of the strengthening phases such as the T_1 phase, GP(2) zone and the θ' phase were measured to determine the effect of Mg addition in Weldalite™049 alloy. The measurement was performed on the bright field TEM images in various aging conditions in Weldalite and Mg-free alloys, assuming the thickness of the TEM foils to be ~ 100 nm. The average precipitate sizes were determined from the size distributions of edge-on precipitates on the $\{011\}_a$ orientations, and the precipitate densities were assessed as the precipitate numbers including other variants per 1cm^3 .

Fig.6 shows the size distribution changes of each strengthening phase produced during aging at 433K, in which the Mg addition exerts the pronounced influence on the aging behavior of Weldalite™049 alloy. It is evident that the small amount of Mg causes the high density precipitation of the T_1 phase at the peak-aging time as 346ks (Fig.6(a)). In contrast, although Mg-free alloy has a rather high precipitate density of fine GP(2) zone, the T_1 phase is not

detected until the time of overaging (1.9×10^4 ks)(Fig.6(b),(c)). This implies that the small amount of Mg is effectively utilized for enhancing nucleation of the T_1 phase, which results in the improved mechanical strength. Pickens *et al.*[9] suggested that local ordering including Ag and Mg atoms could lead to the formation of the T_1 nucleus, as has been shown for the Ω phase in Al-Cu alloys [2]. However, the mechanism for the refined distribution of the T_1 phase is not fully interpreted in terms of the nucleation aids of such fine Mg_3Ag particles because an Ag-free alloy containing identical composition with Weldalite™049 alloy also exhibits the similar marked aging response caused by the homogeneous precipitation of the T_1 phase. The reduction in the peak hardness is only about HV10 under the aging conditions of both 433 and 463K[10].

As the T_1 phase has a hexagonal structure ($a=0.497$ nm and $c=0.935$ nm) with a lattice plane stacking sequence ABABAB..., the stacking faults are inevitably introduced in the fcc structure of aluminum, ABCABABC..., for the nucleation and growth of the T_1 phase. In general, the stacking fault energy of aluminum, a relatively high value of ~ 0.15 Jm⁻², is known to be lowered by trace additions of elements such as zinc, magnesium, lithium, silver and germanium due to their comparatively high solubilities at the usual aging temperatures[11]. Thus, the nucleation and growth of the T_1 phase is considered to be much easier to take place in Mg-containing Weldalite alloy because of the reduced stacking fault energy. However, it is also necessary to investigate in more details the mechanisms of the enhanced nucleation and growth of the T_1 phase by the small addition of Mg from other points of views, i.e. the metastable phase boundaries, the dislocation loops and helices introduced with the excess vacancies.

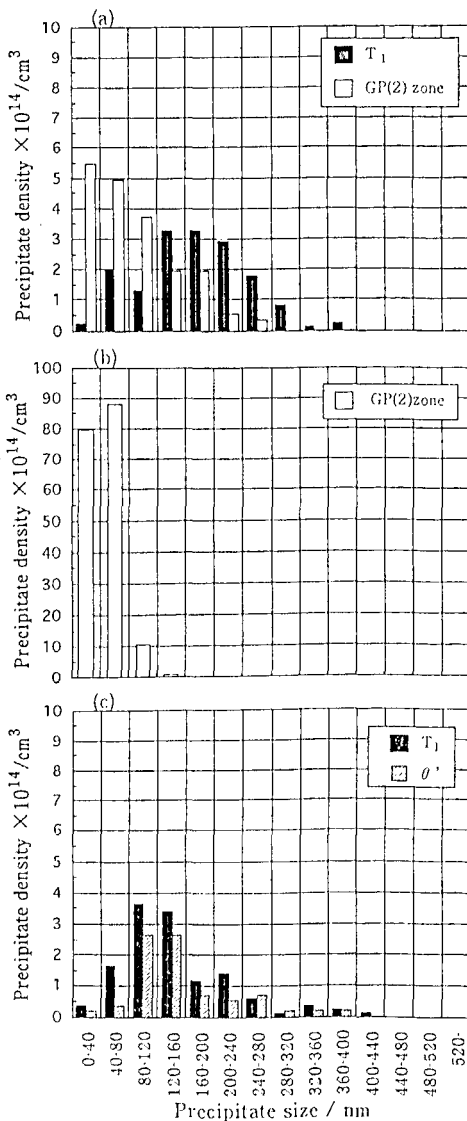


Fig.6 Precipitate size distributions for (a) Weldalite alloy aged at 433K for 346ks and Mg-free alloys aged at 433K for (b) 346ks and (c) 1.9×10^4 ks. Micrographs are shown in Fig.4.

Conclusions

The addition of small amount Mg to Al-Li-Cu-Zr alloys containing Ag, known as Weldalite™049 alloy, significantly exerts an effect on the precipitation hardening over the temperature range from R.T. to 523K. The marked increment of mechanical strength is found to arise from the changes in the precipitation rate of GP(1) zones and the T₁ phases. In the temperature range from R.T. to 373K the small amount of Mg accelerates the formation of GP(1) zones resulting in the faster age-hardening. This can be explained in terms of a decrease in an activation energy for formation of GP(1) zone due to the Cu/Mg/vacancy complexes diffusion. On the other hand, at the more elevated temperatures the Mg addition causes the change in the major strengthening phase from GP zone and/or θ' phase to the T₁ phase, resulting in the marked acceleration of the T₁ phase formation. This is considered to be much easier in the nucleation and growth of the T₁ phase due to not only the nucleation aids of the MgAg particles but also the reduced stacking fault energy caused by the small addition of Mg.

References

1. I.J.Polmear, *Nature*, **186**, (1960),303.
2. J.A.Taylor, B.A.Parker and I.J.Polmear, *Metal Science* **12**, (1978), 478.
3. K.M.Entwistle, J.H.Fell and Kang Il Koo, *J. Inst. Metals*, **91**, (1962-63), 84.
4. R.K.Wyss and R.E.Sanders, Jr., *Metall. Trans.* **19A**, (1988), 2523.
5. A.Kelly and R.B.Nicholson, *Precipitation Hardening*, *Prog. Mater. Sci.* **10**, (1961), 148.
6. A.J.Perry and E.M.Entwistle, *J. Inst. Metals*, **96**, (1968), 344.
7. J.J.Regidor and A.Sanchez, *6th Int. Light Metals Congress*, Leoben, Vienna, Aluminum-Verlag GMBH, Düsseldorf, (1975), 29.
8. A.K.Niessen, F.R.de Boer, R.Boom, P.F.de Châtel and W.C.M.Mattens, *CALPHAD*, **7**, (1983), 51.
9. J.R.Pickens, F.H.Heubaum T.J.Langan and L.S.Kramer, *Proc. 5th Int. Al-Li Conf.*, **Vol.3**, (1987), 1397.
10. A.Kamio, T.Sato, S.Hirosawa, K.Kobayashi and Y.Tsuji, *Proc. 84th Conf. Japan Inst. Light Metals*, (1993), 389.
11. V.D.Scott, S.Kerry and R.L.Trumper, *Mat. Sci. Tech.*, **3**, (1987), 827.